Polymerization shrinkage kinetics and degree of conversion of commercial and experimental resin modified glass ionomer luting cements (RMGICs)

Amani Agha*, Sandra Parker, Mangala Patel

Dental Physical Sciences Unit, Queen Mary University of London, E1 4NS, United Kingdom

Abstract

Objective. Tetrahydrofurfuryl-methacrylate (THFM) and hydroxypropyl-methacrylate (HPM) were used to partially or fully replace HEMA in experimental RMGICs. The experimental materials were compared with home and commercial products in terms of degree of conversion, polymerization shrinkage and exotherm.
Methods. Two commercial RMGICs used were Fuji-Plus (GC, Japan) and RelyX-Luting (RX, 3M-ESPE, USA). Two additional in-house liquids were prepared based on the commercial materials liquids. Eight experimental liquid compositions (F1, F2, F3 and F4 based on Fuji-Plus; R1, R2, R3 and R4 based on RelyX-Luting) were prepared replacing 100% HEMA with HPM in F1 and R1 or HPM/THFM in F2 and R2. 50% HEMA was replaced with THFM in F3 and R3 compared to 30% in F4 and R4. All liquids were mixed with the corresponding commercial powder. Degree of conversion was determined using Fourier-transform infrared spectroscopy (FT-IR). Polymerization shrinkage and exotherm were measured using the bonded-disk method.
Results. Compositions containing HPM (FP and RX) showed lower degree of conversion compared to experimental compositions containing THFM, home and commercial materials ($p<0.0001$). FP-commercial showed significantly higher polymerization shrinkage and exotherm compared to all other materials in both groups ($p<0.0001$). FP-commercial showed higher degree of polymerization shrinkage and exotherm at 5 minutes compared to all materials due to the incorporation of an additional cross-linker (glycerol-dimethacrylate). In general, compositions containing THFM, presented polymerization shrinkage and degree of conversion values similar to their corresponding commercial products.
Significance. THFM monomer showed promising results and could be potentially useful in the development of new RMGICs with improved properties.

Keywords: Resin-modified glass ionomer, degree of conversion, polymerization shrinkage, polymerization exotherm, hydroxyethyl methacrylate, tetrahydrofurfuryl-methacrylate, hydroxypropyl-methacrylate.

1 Introduction:

Dimensional stability of dental cements is an important feature that can affect the longevity of the restoration. Shrinkage that occurs following application of the material can lead to marginal gaps and leakage, which could lead to secondary caries, and contribute to the failure of the restoration (1). Shrinkage of resin-based dental materials is directly associated with the percentage degree of conversion of the carbon-carbon double bonds to single bonds following polymerization (2). The occurrence of polymerisation shrinkage is a result of the change in the molecular bonds (from van-der Waals forces to covalent single bonds) and in the distances between atoms (3). This reaction is also exothermic and, in the case of light activated products, there can be extra heat generated from the light curing device (4).

Resin modified glass ionomer cements (RMGICs) set by both an acid-base reaction, similar to the conventional glass ionomer cements (GICs), and polymerisation of the monomer (commonly used is hydroxyethyl methacrylate; HEMA). GICs do not undergo polymerisation shrinkage and have a 'very low to non-existent reaction exotherm' (5, 6). However, due to the fact that RMGICs contain HEMA and undergo polymerisation (light and/or chemically), a degree of polymerisation shrinkage and a rise in temperature on setting, are commonly associated with this type of cement (7). Although it is favorable to increase the degree of conversion (polymerization) of dental materials in order to enhance their mechanical and biological properties (8), a high degree of conversion is less desirable due to the possibility of increasing polymerization shrinkage, exotherm and brittleness of the material (7, 9).

The larger the molar volume of the monomer, the fewer monomer units are required to be converted for the same volume of material (10, 11). Therefore, in theory, in order to achieve RMGICs with a higher degree of conversion, but with clinically acceptable polymerization shrinkage, monomers with higher molecular weights and molar volume could be used (12). Tetrahydrofurfuryl methacrylate (THFM) has been studied for use in RMGICs, where it partially replaced HEMA and this resulted in improved properties (water uptake and

dimensional change) (13). Another monomer that could be used to replace HEMA is hydroxyl propyl methacrylate (HPM), which is the next member in the homologous series, just below HEMA, which contains an extra CH_2 group between the hydroxyl and methacrylate groups. It has a lower setting exotherm and reduced water uptake compared to HEMA (14). Both HPM and THFM have higher molecular weights and higher molar volumes compared to HEMA. Thus it can be assumed that they may demonstrate lower shrinkage and higher degree of conversion values (12).

The polymerization process can be characterized by Fourier Transform Infra-Red Spectroscopy (FT-IR) as this technique is based on the absorption of radiation of the functional groups in the polymer chain, and their molecular vibration in the infrared frequency range (15). Moreover, this technique (FT-IR) can be used to calculate the degree of conversion of resin composites by measuring the ratio of absorbance intensities of the aliphatic carbon–carbon double bond (C=C), at ~1638 cm^{-1}, and aromatic double bond (C=C) at ~1609 cm^{-1} (16, 17). However, a study by Young et al. (2002) showed that the peak at 1638 cm^{-1} could not be used to quantify the degree of conversion in RMGICs since the formulation contains water, which absorbs at this wavenumber, thus making it difficult to determine the peak base at this point. Therefore, a different peak was used (at 1320 cm^{-1}) and, the degree of conversion results obtained using this peak, were in agreement with those obtained from Raman studies (18, 19).

The polymerization shrinkage strain can be measured using the bonded-disk method, which was first mentioned by Walls et al. and Bausch et al. (20, 21) and further developed by Watts and Cash (22). This technique was subsequently improved and modified by Watts and Hindi (23). The shrinkage strain of the material is measured using the bonded-disk method after applying the mixed material onto a rigid glass plate (3mm thickness), which consequently bonds to one surface of the glass maintaining a constant dimension of the circumference at 8mm diameter (24). Watts and Cash demonstrated that no change occurred in the circumference of the tested material as a result of bonding to the glass plate; hence shrinkage occurred only in

the vertical plane, in the unbound surface (22). Therefore, the measurement of the strain (ε) in the axial plane corresponds to a close approximation to the volumetric strain of the material. Another advantage of this technique is that the polymerisation exotherm can be measured simultaneously, since a thermocouple can be inserted in the material during the measurement of shrinkage.

Therefore, the objectives of this study are to:

- Analyse the composition and setting reactions of commercial and experimental RMGICs using FT-IR, and moreover to measure and compare the degree of monomer(s) conversion by comparing the absorbance peak immediately and 30 minutes after mixing.
- Measure and compare the percentage polymerisation shrinkage and exotherm simultaneously of commercial and experimental RMGICs in order to determine the effect of replacing HEMA, fully or partially, with higher molar volume monomers.

2 Materials and Methods

2.1 Materials

Two commercial chemically cured resin modified glass-ionomer cements (RMGICs) were included in this study, namely Fuji Plus (FP, GC Corporation, Tokyo, Japan) and RelyX Luting (RX, 3M ESPE, St Paul, MN, USA). Two additional control liquids were prepared in-house (FP home and RX home), based on the corresponding commercial liquid composition, and these were to be mixed with the corresponding commercial powders.

Eight experimental liquid formulations were prepared for this study, four for each of the commercial products (RX, FP), where HEMA was replaced with either 100% HPM (F1 and R1), 70%/30% HPM/THFM (F2 and R2), 50%/50% THFM/HEMA (F3 and R3) and 30%/70% THFM/HEMA (F4 and R4). All experimental and home liquids were mixed with the corresponding commercial powder.

2.2 Methods

2.2.1 FT-IR analysis technique:

All commercial, home and experimental materials (unset liquids and set materials) were tested using FT-IR spectrometer (Perkin Elmer series 880) supplied with a Golden Gate Single Reflection Diamond attenuated total reflectance (ATR) accessory (Graseby Specac Ltd, Kent, UK). A total of 144 FT-IR spectra were obtained divided as four spectra taken at four time points (at 0, 5, 10 and 30 minutes), from the start of mixing for all commercial, home and experimental cements (n=3 per material). Furthermore, the corresponding FT-IR spectra were compared and analysed with spectra obtained from known monomers (n=3).

Spectra of absorbance versus wavenumber were obtained at a resolution of 4 cm^{-1} and, 10 scans in the range of 4000-500 cm^{-1}, were used to determine the absorbance peaks of the materials before and after curing.

For identification of degree of polymerisation, materials were mixed at room temperature (23 ± 1°C) according to the manufacturers recommended powder: liquid mixing ratio (2:1 g:g for FP group and 1.6:1 g:g for RX group). In order to standardise the amount of RMGIC investigated, a wax ring of 8mm diameter and 1.5mm thickness was prepared using a profile wax stick (Berg Dental, Engen, Germany) and placed on the ATR accessory with the ATR crystal in the middle of the wax ring. The mixture was then placed inside the wax ring; the top surface was covered with an acetate sheet and a scan was run as zero time. After 10 minutes from the start of mixing, pressure was applied to the top surface of the sample using the compression head anvil in the ATR, in order to maintain good contact with the crystal. Subsequent spectra were generated at 0, 5, 15 and 30 minutes from the start of mixing thereafter. The analysis was repeated 3 times for all materials at each time point.

2.2.2 Treatment of FT-IR data

The peak height at 1320 cm^{-1} was used to quantify the degree of conversion (DC) of the monomer by measuring the net peak height difference between the absorption from 0 time (A_0) to 30 minutes later (A_t). Equation 1 was used to calculate the degree of conversion.

$$DC\ (\%) = (A_0 - A_t)/A_0 \times 100 \qquad \text{(Equation 1)}$$

Degree of conversion values calculated at each time point (5, 10 and 30 minutes) were compared between all materials for a significant difference using one-way ANOVA followed by post-hoc Tukey test at significance level of p=0.05.

2.2.3 Polymerization shrinkage strain and exotherm:

Polymerisation shrinkage strain was measured using the bonded-disk instrument, which was calibrated prior to starting the shrinkage experiment. The experiment was conducted in a temperature-controlled instrument at both 23 ± 1°C and at 37 ± 1°C, the latter to mimic the oral environment temperature. The instrument was switched on and left to equilibrate in temperature for 2 hours prior to starting the testing.

The instrument consists of a linear variable displacement transducer (LVDT - sensitivity greater than 0.1 μm), fixed to an aluminium stand above a brass anvil (40mm diameter). The experiment assembly (16 ± 0.1mm diameter and 1 ±0.1mm thickness square cross sectioned), comprised a brass ring bonded centrally on a glass slide (74mm length, 25mm width and 3mm thickness. The glass slide and brass ring was covered with a square microscope cover slip (22x22mm area and 0.13mm thickness; Number.0, VWR International, Radnor, PA, USA). The whole assembly was placed centrally on a temperature controlled metal plate and specimen platform, so that the LVDT was lightly in contact with the centre of the flexible cover slip. The movement of the cover slip was detected by the LVDT. The latter was connected to a signal-controlling unit (E309, RDP Electronics, Wolverhampton, UK) that transferred the data to a

computer through a data logging system hardware and software (ADC-20 multichannel unit and Pico-log software, Picotech, Cambridge, UK).

In order to measure the polymerization exotherm simultaneously, a thermocouple was passed through a carefully drilled groove in the centre of the glass slide reaching the centre of the brass ring. The end of the thermocouple was placed centrally in the test material. This thermocouple was attached to a type-K thermocouple amplifier (TCK-4, Audon Electronics, Nottingham, UK) which transferred the exotherm data to the ADC-20 unit.

2.2.4 Treatment of shrinkage strain data:

A total of 60 samples divided into 12 groups (n=5) of different compositions (commercial, home and experimental) were investigated for polymerisation shrinkage strain and exotherm using bonded-disk technique.

The final specimen thickness (L) was measured using a digital micrometre accurate to 10μm. The calibration coefficient of displacement/voltage was used to calculate the displacement of the cover slip during the experiment (dL), which was then used to determine the original specimen thickness (L_0) in μm, following Equation 2.

$$L_0 = dL + L \qquad \text{(Equation 2)}$$

The percentage shrinkage strain was calculated using Equation 3. These values were then plotted against time (seconds) to originate the shrinkage strain kinetic curve from the start to the end of the experiment.

$$\text{Shrinkage strain \%} = (dL / L0) * 100 \qquad \text{(Equation 3)}$$

2.2.5 Treatment of shrinkage exotherm data:

The maximum temperature reached was recorded and compared for significant differences between the materials using one-way ANOVA followed by post-hoc Tukey test at a significant

level of p=0.05. Moreover, the time to reach the peak temperature was also recorded as the period from the start of mixing to the time required to reach the maximum temperature.

3 Results

3.1 Composition analysis:

Table 1 and figure 1 summarise FT-IR wavenumbers of PAA, water and all monomers used in the commercial, experimental and home liquids. The only difference between the spectra of RX and FP liquids was the additional peaks at 1059 cm^{-1} (C-N stretch), 1250 and 1535 cm^{-1} (N-H bond), representing UDMA in FP liquid compositions (~4%). Peaks at 1631 cm^{-1} and at 1701 cm^{-1} represent C=C and C=O group respectively, and peaks at 1301 cm^{-1} and 1324 cm^{-1} refer to the C-O stretch in monomers (19). Tartaric acid (peak at 1086 cm^{-1}) was present at 5-10%, according to the manufacturer's material's safety data sheet (MSDS) in commercial materials, and at 5% in the home and experimental liquids. HPM showed an additional peak at 1059 cm^{-1} corresponding to the C–OH group in its structure, while HEMA and THFM showed additional peaks at ~1020 and 1086 cm^{-1}, corresponding to the C–O–H group in HEMA's structure and the ring stretch in THFM (25, 26).

Figures 1c and 1d show the FTIR spectra of experimental liquid compositions in the FP and RX groups respectively (between wavenumbers of 800 cm^{-1} and 1800 cm^{-1}). Compositions of cements containing HPM, from both groups (F1, F2, R1 and R2), showed an additional peak at ~1059 cm^{-1} representing the C–OH stretch. Moreover, peaks at ~1084 cm^{-1} were sharper in compositions containing THFM and HEMA (F3, F4, R3, R4).

3.2 Analysis of Reaction

According to the literature (discussed in the introduction), regarding the measurement of degree of conversion concerning RMGIC, the peak at 1320 cm^{-1} was used instead of 1638 cm^{-1}. 1720 cm^{-1} was used as a reference peak. The degree of conversion results obtained using this peak, were in agreement with those obtained from Raman studies (18, 19).

Figures 2a and 2b are representative FT-IR spectra taken during the setting of Fuji Plus commercial and home respectively, as soon as the cement was applied to the ATR crystal (0 minutes) and at 5, 10 and 30 minutes, from the start of mixing. As can be seen in Figure 2a, changes in absorbance occurred in FP (commercial) in the 5 minutes' spectrum when compared to that at 0 minutes. These changes included loss of C=C at 1630 cm^{-1}, 1320 and 1300 cm^{-1} and a shift of the latter two wavenumbers to 1275 and 1253 cm^{-1}. Small changes also occurred at 1700 and 975 cm^{-1} representing C=O and glass Si-O stretch respectively (27). These changes also occurred in FP Home (Figure 2b) but at later time points, thus indicating a slower reaction.

Spectral changes due to the acid-base reaction were detected, due to the formation of 1400, 1492 and 1563 cm^{-1} peaks, which can be assigned to the polyacrylate salts formed (C=O stretching of Ca-polyacrylate, Al-polyacrylate, Ca-polyacrylate respectively) (27). Again, a faster reaction occurred in FP compared to FP home.

Figures 2c and 2d represent the FT-IR spectra taken at 0, 5, 10 and 30 minutes during the setting of RX and RX home respectively, from the start of mixing. Main changes in the spectra occurred following 5 minutes from the start of mixing, where the peaks at 1300 and 1320 cm^{-1} were still visible, but at lower absorbance values. These two peaks shifted to 1264 and 1285 cm^{-1} at 5 minutes but had higher absorbance values at 10 and 30 minutes. Similar to FP and FP home spectra, the peak at 1638 cm^{-1} disappeared as a result of the setting reaction and the conversion of the methacrylate C=C bond to C-C.

Glass and polyacrylate peaks at 970, 1405, 1480 and 1556 cm^{-1} were observed from the 5 minutes time points, which increased in intensity from 10 minutes.

RX home spectrum, presented in Figure 2d, showed a slower polymerisation reaction compared to RX commercial. In both spectra, peaks at 1300 and 1320 cm^{-1} shifted to 1264 and 1285 cm^{-1}, and there was a difference in the time the shifts occurred (5 minutes in RX and 10 minutes in RX home). These two peaks were used to calculate the degree of conversion of monomer in the

cements. There were signs of the acid-base reaction occurring in RX commercial and home materials following 10 minutes.

Figures 3 and 4 (a,b,c and d) are representatives of the spectra obtained during the setting reaction of experimental FP and RX cements respectively. As can be seen in Figure 3, the F3 spectrum (3c) was different compared to all other materials in the FP group with respect to the loss of methacrylate group peaks (at 1300 and 1320 cm^{-1}), which shifted to 1264 and 1280 cm^{-1} at 5 minutes. In all other FP group materials, the former peaks shifted after 10 and 30 minutes similar to all RX compositions (Figure 4). Moreover, the spectrum also shows the formation of GIC salts and neutralisation of the acid (at 1550, 1484 and 1402 cm^{-1} COO^- stretch) in F3 at 5 minutes compared to later time points for other materials in the same group. This possibly indicates that the reaction is occurring faster in F3 compared to the other materials.

Percentage degree of conversion of commercial, home and experimental materials:

Figure 5a shows the mean percentage degree of conversion of FP commercial, home and experimental materials in the FP group, calculated as the change in peak height of the methacrylate group in each cement at 5, 10 and 30 minutes from the start of mixing. At 5 minutes interval, F3, FP and FP-Home showed statistically higher degree of conversion values (33.75 ± 4.25%, 28.12 ± 2.13% and 21.92 ± 9.46% respectively) compared to F4, F1 and F2 (14.91 ± 2.12%, 7.80 ± 3.01 and 6.58 ± 1.27% respectively; $p \leq 0.039$). F3, FP-Home, FP and F4 showed statistically comparable degree of conversion values at 10 minutes from the start of mixing (33.50 ± 3.83%, 33.12 ± 3.63%, 31.63 ± 1.32% and 25.94 ± 5.93%) ($p \leq 0.73$). The degree of conversion values at 10 minutes for F2 and F1 were the lowest in the FP group (18.79 ± 5.80% and 14.26 ± 4.93%; $p \leq 0.002$); there was no significant difference between degree of conversion values at 10 minutes and 30 minutes of each material.

Figure 5b shows the mean percentage degree of conversion of RX commercial, home and experimental materials in the RX group. Only R1 showed a significantly lower degree of

conversion (9.47 ± 1.86%) compared to the commercial RX (23.15 ± 5.84%; p=0.029) at 5 minutes, but this was not significantly different compared to all other materials in the group (R3 - 17.10 ± 2.76%, RX-Home - 14.90 ± 5.81%, R2 - 14.63 ± 2.19% and R4 - 13.62 ± 4.09%; p≤0.987). Following 10 minutes from the start of mixing, RX and R4 showed significantly higher monomer conversion (37.02 ± 1.91% and 34.08 ± 3.22%) compared to R2 and R1 (24.74 ± 0.01% and 22.84 ± 1.68%; p≤0.004), but they were not significantly different compared to R3 and RX-Home (31.13 ± 0.48% and 30.95 ± 3.96%; p≤0.79). Similar trends were noticed in the degree of conversion values at 30 minutes' intervals in the RX group.

3.3 Polymerization shrinkage strain at 23 °C:

Mean percentage shrinkage strains (n=5) 23 °C of FP and RX are summarised in Tables 2 and 3 respectively for measurements taken at 5, 15, 30 and 60 minutes.

At 23°C, five minutes from the start of measuring shrinkage, commercial FP showed the highest shrinkage, which was significantly different compared to all materials in the group (home and experimental; p<0.0001). Interestingly, shrinkage values for compositions containing HEMA (F3, FP-Home and F4) were significantly lower than commercial FP (also containing HEMA) at this time point (p<0.0001); furthermore, they were significantly higher than the compositions containing HPM (F1; p<0.0001) and, composition F2, where HEMA was replaced by 30% THFM and 70% HPM (p<0.0001). F1 presented with a significantly lower shrinkage at this time point compared to all materials in this group (p≤0.041), and to all materials at all-time points (p≤0.041), except when compared to F3 at 60 minutes (p=0.146). FP and FP-Home showed statistically similar results at 15, 30 and 60 minutes (p≥0.822) (Table 2).

RX-Home presented with the lowest shrinkage strain values, which were statistically significant from most of the other materials in the group, especially at earlier time points (5 and 15 minutes) (Table3). All experimental materials in the RX group (R1, R2, R3 and R4) had statistically comparable shrinkage values compared to commercial RX, at all-time points, at 23°C (p≥0.526).

3.4 Polymerization shrinkage strain at 37 °C

Similar to the polymerisation shrinkage behaviour at 23°C, FP showed the highest shrinkage at 5 minutes, which was significantly different from all materials in the FP group ($p \leq 0.037$). Following 60 minutes from the start of the shrinkage measurement, all materials in the FP group showed statistically comparable shrinkage values ($p=0.085$) (Table 4).

At 37°C, materials in the RX group showed a similar trend in the polymerisation shrinkage data to RX commercial, at different time points; there were no significant differences in shrinkage between all materials (commercial, home, and experimental) ($p \leq 1$). This was also noted for all RX materials when the experiment was performed at 23°C.

3.5 Polymerization exotherm

FP commercial had a significantly higher exotherm at 23°C compared to all materials in the group ($p<0.0001$), and it also reached this exotherm faster than other materials, except for F4 ($p=0.864$). Although there was a statistically significant difference in reaching the peak temperature for FP-Home, F4 and F2 ($p<0.0001$), all three presented with comparable exotherm results ($p=0.896$). F1 increased in temperature by only 0.81 ± 0.12°C, which was significantly lower than all other materials in the group ($p \leq 0.003$). Moreover, F1 took more time to reach this temperature, compared to the other materials ($p<0.0001$), with the exception of F2 ($p=0.427$) (Table 6).

A similar trend in the exotherm was noted at 37°C in that FP commercial had a significantly higher exotherm compared to all materials in the group ($p<0.0001$) and, moreover, less time was needed to reach this temperature ($p \leq 0.001$). However, the exotherm noted at 37°C was ~ 43% higher than that recorded at 23°C, reaching 6.12 ± 0.48°C, as a result of the polymerisation reaction. F1 exhibited a lower exotherm but the value recorded at 37°C was not significantly different to F4 and F2 values ($p=0.301$). There was no significant difference between the

exotherms at 37°C (p=0.068) for compositions containing HEMA (FP-Home, F3 and F4; Table 7).

The only significant difference between materials, with respect to exotherm data, measured at 23°C, was found between RX and R3 (p=0.013), despite these two materials showing similar results in their time taken to reach the maximum temperature recorded (p=0.563). R1 required a significantly longer time than all other materials in the same group to reach the maximum temperature recorded, except when compared to RX (p=0.064; Table 8). Mean peak exotherm temperatures for RX materials at 37°C ranged from 1.82 to 2.07°C (Table 9). Following one-way ANOVA testing, there was no significant difference between the peak exotherm of all materials in this group (p=0.491). Despite this, RX required significantly less time to reach the peak temperature compared to all materials (home and experimental) in the same group (p<0.0001; Table 9).

4 Discussion:

RMGICs contain components required for both the acid-base and polymerization reactions to occur. In this study, all materials were chemically activated and thus the two reactions occurred simultaneously following mixing. Spectra of commercial, home and experimental materials showed acid neutralization peaks (indicating that the acid- base reaction had taken place) at 1550, 1484 and 1402 cm-1. The difference in the monomer compositions of FP and RX (commercial, home and experimental materials) was the inclusion of UDMA in FP.

As discussed earlier (Introduction), commonly the peaks used to identify resin materials' degree of conversion in literature were at 1638 cm^{-1} and 1712 cm^{-1} (reference peak) (28, 29) (Kakaboura *et al.*, 1996; dos Santos *et al.*, 2012). These peaks could not be used in this study, since the peak at 1638 cm^{-1} was masked by the presence of water (in the material) that also absorbs at the same wavelength. Therefore, the DC was calculated using the peak at 1320 cm^{-1}, as reported by Young et al. (19).

The analyses of reactions (both acid-base and polymerization of the monomer) showed that the setting reaction occurred faster (by five minutes) in both commercial cements (FP and RX) compared to the home materials. Despite this time difference, and using different peaks to identify the polymerization reaction, there was no statistically significant difference between commercial and home materials with respect to the calculated degree of conversion of the methacrylate monomers, at all-time intervals; they also showed agreement with other studies on RMGIC in that the percentage maximum conversion occurred mainly in the first 10 minutes, following mixing or light activation (30-32). According to Young (2002), differences in water content and the acids used in the products could affect the acid-base reaction times (18). Therefore, the differences between commercial RX and RX Home could be a result of the different acids used [(copolymer of acrylic and itaconic acid compared with poly(acrylic acid), respectively)].

In both groups (FP and RX), compositions containing HPM instead of HEMA, showed a lower degree of conversion. It was reported that an increase in viscosity and slower movement in the matrix occur respectively with increasing the molecular weight of a monomer (10, 33). HPM contains an additional CH_2 compared to HEMA and therefore, it has a higher molecular weight. Hence this may have caused the lower degree of conversion values in this study. Another article (14) reported that THFM, partially replaced with either HEMA or HPM, showed reduced reactivity of a system containing HPM, compared to a similar system containing HEMA.

The bonded disk method was used to measure the polymerization shrinkage strain of all materials. It recorded the axial movement and shrinkage of the material in one direction, since the bottom surface of the specimen was directly attached to the 3mm thickness glass plate. This validated method was used to calculate the percentage shrinkage strain of each specimen, since it has been used previously for a variety dental materials, including resin composites, impression materials, GICs and RMGICs (22-24, 34-36).

Shrinkage strain (shrinkage) data for F1 and F2 (compositions containing HPM), at 23°C, showed lower percentage shrinkage. This data agrees with the degree of conversion results, measured by FT-IR, which showed a lower degree of conversion for F1 and F2, compared to other materials in the same group. Hence, the degree of shrinkage could also give an indication of the degree of polymerization in the material (10), since shrinkage is a result of the change of van-der-Waals forces to covalent single bonds in the methacrylate system. Differences in polymerization shrinkage were observed between 23°C or 37°C, in the FP group materials in the first 5 minutes of the experiment. This could be a result of the increased mobility of the monomers at 37°C compared to 23°C, which allowed for the reaction to occur faster. Therefore, more double bonds were converted to single bonds, subsequently resulting in higher shrinkage values at 37°C, which agree with published literature (23).

All materials in the RX group (commercial, home and experimental) did not show any significant differences between each other at 37°C and 23°C, with the exception of RX Home at 23°C, which demonstrated significantly lower shrinkage values at this temperature. This could be a result of the material exhibiting an expansion prior to shrinking, which may have affected the results obtained.

The polymerization reaction of monomers in dental materials generates heat (exotherm) following the conversion of the carbon-carbon double bonds to single bonds. This reaction occurs as a result of the initiation procedure that can be generated through heat, light or at room temperature (37). In this study, the reaction was initiated chemically (at room temperature), where in the presence of water, ascorbic acid reacted with potassium persulphate generating free radicals that then reacted with the monomer, to convert the double bonds into single bonds (38). The latter resulted in heat generation, which further enhanced the polymerization reaction and moreover increased the heat generated.

The polymerization of monomers (in dental materials) in situ results in the generation of heat, which can cause 100% irreversible pulpal damage when the exotherm reaches 16.6°C (39).

Therefore, reducing the polymerization exotherm of dental materials is highly desirable. In this study, the exotherm of all materials was studied at both 37 ± 1°C (body temperature) and at ambient temperature of 23 ± 1°C, which was of clinical importance, due to the fact that although the body temperature is 37°C, the oral cavity baseline temperature has been recorded as 25.1°C with rubber dam application (40).

According to Hanning and Bott, a temperature rise in light-cured dental cements is a result of the exotherm occurring from the light source and the polymerization reaction itself (41). However, in this study, the exotherm was solely a result of the polymerization reaction since all materials were chemically activated. At both temperatures, commercial FP showed a higher exotherm than home and experimental materials, which although theoretically should agree with the degree of conversion values, as the heat produced is a result of the change in the C=C double bond to single bonds, it did not. One explanation for this is that commercial FP contained an additional monomer (glycerol dimethacrylate) that also polymerizes, which was not present in the home and experimental FP materials. Therefore, the higher temperature of commercial FP could be due to the conversion of this additional monomer. Experimental F1 and F2 had lower exotherms at both temperatures (compared to other materials in the FP group); this data agrees with the corresponding degree of conversion and shrinkage results for F1 and F2, since they had lower shrinkage strain and degree of conversion, particularly F1.

The FP group had higher exotherms compared to the RX group. This could be due to the composition of FP containing UDMA in addition to the other monomers in the cement (HEMA, THFM and HPM), whereas RX did not. UDMA monomer is a dimethacrylate containing C=C (vinyl group) at each end of the molecule, which took part in the polymerization reaction. Since the exotherm is dependent on the conversion of the double bond, also as mentioned earlier, this can justify the higher exotherm temperature of the FP group.

Similar to the shrinkage strain results, all RX materials did not show any significant differences between each other with respect to exotherm. However, this does not agree with the degree of

conversion results. It was expected that the RX compositions containing HPM would have a significantly lower exotherm compared to all other materials in that group since they showed a lower degree of conversion. This may be due to the very low temperature increases recorded for this group, and therefore, the significancy between materials could not be calculated.

5 Conclusion:

Further improvement on the degree of conversion with compositions containing HPM need to be considered, by for example, including a higher percentage of the dimethacrylate monomer (e.g. UDMA) and/or glycerol dimethacrylate, to enhance crosslinking of the matrix. However, exotherm and shrinkage should also be taken into consideration.

Interestingly compositions containing THFM monomer showed promising results, with a comparable degree of conversion, polymerization shrinkage and exotherm compared with commercial and home materials. Hence, THFM monomer (partially replacing HEMA) emerges as a potentially useful candidate in the development of new RMGICs with improved properties.

6 References

1. Qvist V. Resin restorations: leakage, bacteria, pulp. Endodontics & dental traumatology. 1993;9(4):127-52.

2. Anusavice KJ, Phillips RW, Shen C, Rawls HR. Phillips' Science of Dental Materials: Elsevier/Saunders; 2012.

3. Yoon TH, Lee YK, Lim BS, Kim CW. Degree of polymerization of resin composites by different light sources. J Oral Rehabil. 2002;29(12):1165-73.

4. McCabe JF. Cure performance of light-activated composites by differential thermal analysis (DTA). Dent Mater. 1985;1(6):231-4.

5. Sidhu SK, Watson TF. Resin-modified glass ionomer materials. A status report for the American Journal of Dentistry. Am J Dent. 1995;8(1):59-67.

6. Brook IM, Hatton PV. Glass-ionomers: bioactive implant materials. Biomaterials. 1998;19(6):565-71.

7. Kanchanavasita W, Pearson GJ, Anstice HM. Factors contributing to the temperature rise during polymerization of resinmodified glass-ionomer cements. Biomaterials. 1996;17(24):2305-12.

8. Du M, Zheng Y. Degree of conversion and mechanical properties studies of UDMA based materials for producing dental posts. Polymer Composites. 2008;29(6):623-30.

9. Stansbury JW, Trujillo-Lemon M, Lu H, Ding X, Lin Y, Ge J. Conversion-dependent shrinkage stress and strain in dental resins and composites. Dent Mater. 2005;21(1):56-67.

10. Atai M, Watts DC, Atai Z. Shrinkage strain-rates of dental resin-monomer and composite systems. Biomaterials. 2005;26(24):5015-20.

11. Kim SH, Watts DC. Polymerization shrinkage-strain kinetics of temporary crown and bridge materials. Dent Mater. 2004;20(1):88-95.

12. Patel MP, Braden M, Davy KW. Polymerization shrinkage of methacrylate esters. Biomaterials. 1987;8(1):53-6.

13. Agha A, Parker S, Patel MP. Development of experimental resin modified glass ionomer cements (RMGICs) with reduced water uptake and dimensional change. Dental Materials. 2016;32(6):713-22.

14. Patel MP, Johnstone MB, Hughes FJ, Braden M. The effect of two hydrophilic monomers on the water uptake of a heterocyclic methacrylate system. Biomaterials. 2001;22(1):81-6.

15. Koenig J. Fourier transform infrared spectroscopy of polymers. Spectroscopy: NMR, Fluorescence, FT-IR. Advances in Polymer Science. 54: Springer Berlin Heidelberg; 1984. p. 87-154.

16. Ribeiro BCI, Boaventura JMC, de Brito-GonÇAlves J, Rastelli ANdS, Bagnato VS, Saad JRC. Degree of conversion of nanofilled and microhybrid composite resins

photo-activated by different generations of LEDs. Journal of Applied Oral Science. 2012;20(2):212-7.

17. Galvão MR, Caldas SGFR, Bagnato VS, de Souza Rastelli AN, de Andrade MF. Evaluation of degree of conversion and hardness of dental composites photo-activated with different light guide tips. European Journal of Dentistry. 2013;7(1):86-93.

18. Young AM. FTIR investigation of polymerisation and polyacid neutralisation kinetics in resin-modified glass-ionomer dental cements. Biomaterials. 2002;23(15):3289-95.

19. Young AM, Rafeeka SA, Howlett JA. FTIR investigation of monomer polymerisation and polyacid neutralisation kinetics and mechanisms in various aesthetic dental restorative materials. Biomaterials. 2004;25(5):823-33.

20. Walls AW, McCabe JF, Murray JJ. The polymerization contraction of visible-light activated composite resins. J Dent. 1988;16(4):177-81.

21. Bausch JR, de Lange K, Davidson CL, Peters A, de Gee AJ. Clinical significance of polymerization shrinkage of composite resins. Journal of Prosthetic Dentistry. 1982;48(1):59-67.

22. Watts DC, Cash AJ. Determination of polymerization shrinkage kinetics in visible-light-cured materials: methods development. Dental Materials. 1991;7(4):281-7.

23. Watts DC, Hindi AA. Intrinsic 'soft-start' polymerisation shrinkage-kinetics in an acrylate-based resin-composite. Dental Materials. 1999;15(1):39-45.

24. Watts DC, Marouf AS. Optimal specimen geometry in bonded-disk shrinkage-strain measurements on light-cured biomaterials. Dental Materials. 2000;16(6):447-51.

25. Stepanian SG, Reva ID, Radchenko ED, Sheina GG. Infrared spectra of benzoic acid monomers and dimers in argon matrix. Vibrational Spectroscopy. 1996;11(2):123-33.

26. Rivera-Armenta JL, Martínez-Hernández AL, Mendoza-Martínez AM, Velasco-Santos C, Flores-Hernández CG, Angel-Aldana RZD. Evaluation of Graft Copolymerization of Acrylic Monomers Onto Natural Polymers by Means Infrared Spectroscopy: INTECH Open Access Publisher; 2012.

27. Fareed MA, Stamboulis A. Effect of Nanoclay Dispersion on the Properties of a Commercial Glass Ionomer Cement. International Journal of Biomaterials. 2014;2014:10.

28. Kakaboura A, Eliades G, Palaghias G. An FTIR study on the setting mechanism of resin-modified glass ionomer restoratives. Dent Mater. 1996;12(3):173-8.

29. dos Santos RL, Pithon MM, Martins FO, Romanos MT, Ruellas AC. Evaluation of cytotoxicity and degree of conversion of glass ionomer cements reinforced with resin. European journal of orthodontics. 2012;34(3):362-6.

30. Rueggeberg FA, Caughman WF. The influence of light exposure on polymerization of dual-cure resin cements. Operative dentistry. 1993;18(2):48-55.

31. Yan YL, Kim YK, Kim KH, Kwon TY. Changes in degree of conversion and microhardness of dental resin cements. Operative dentistry. 2010;35(2):203-10.

32. Kim YK, Kim K-H, Kwon T-Y. Setting Reaction of Dental Resin-Modified Glass Ionomer Restoratives as a Function of Curing Depth and Postirradiation Time. Journal of Spectroscopy. 2015;2015:8.

33. Abed YA, Sabry HA, Alrobeigy NA. Degree of conversion and surface hardness of bulk-fill composite versus incremental-fill composite. Tanta Dental Journal. 2015;12(2):71-80.

34. Tolidis K, Nobecourt A, Randall RC. Effect of a resin-modified glass ionomer liner on volumetric polymerization shrinkage of various composites. Dent Mater. 1998;14(6):417-23.

35. Watts DC, Marouf AS. Optimal specimen geometry in bonded-disk shrinkage-strain measurements on light-cured biomaterials. Dent Mater. 2000;16(6):447-51.

36. Bryant RW, Mahler DB. Volumetric contraction in some tooth-coloured restorative materials. Australian dental journal. 2007;52(2):112-7.

37. Ferracane JL. Polymeric materials: the basics. Materials in Dentistry: Principles and Applications. 2nd ed. Lippincott Williams & Wilkins; 2001. p. 255-80.

38. Antonucci JM, Grams CL, Termini DJ. New initiator systems for dental resins based on ascorbic acid. Journal of dental research. 1979;58(9):1887-99.

39. Zach L, Cohen G. PULP RESPONSE TO EXTERNALLY APPLIED HEAT. Oral Surg Oral Med Oral Pathol. 1965;19:515-30.

40. Plasmans PJ, Creugers NH, Hermsen RJ, Vrijhoef MM. Intraoral humidity during operative procedures. J Dent. 1994;22(2):89-91.

41. Hannig M, Bott B. In-vitro pulp chamber temperature rise during composite resin polymerization with various light-curing sources. Dent Mater. 1999;15(4):275-81.

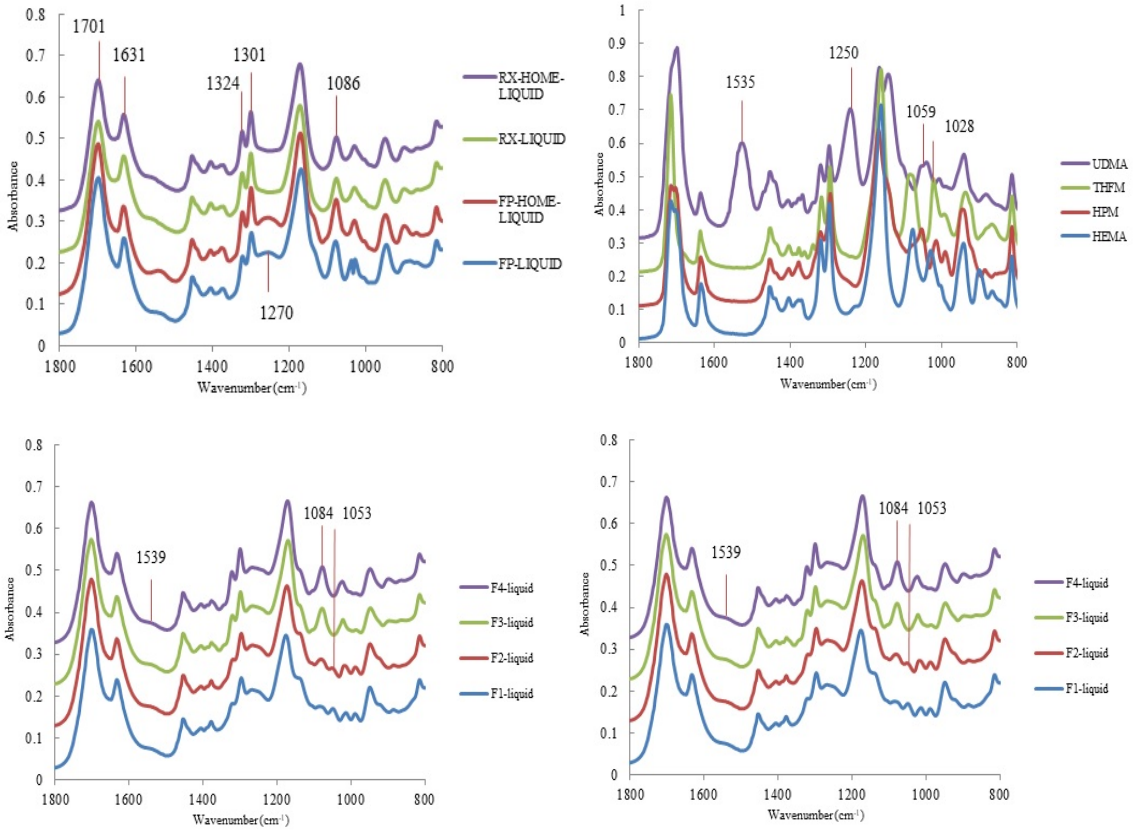

Figure 1 FT-IR spectra of a: commercial and home liquids, b: monomers used in home liquids, c: experimental FP liquids and d: experimental RX liquids.

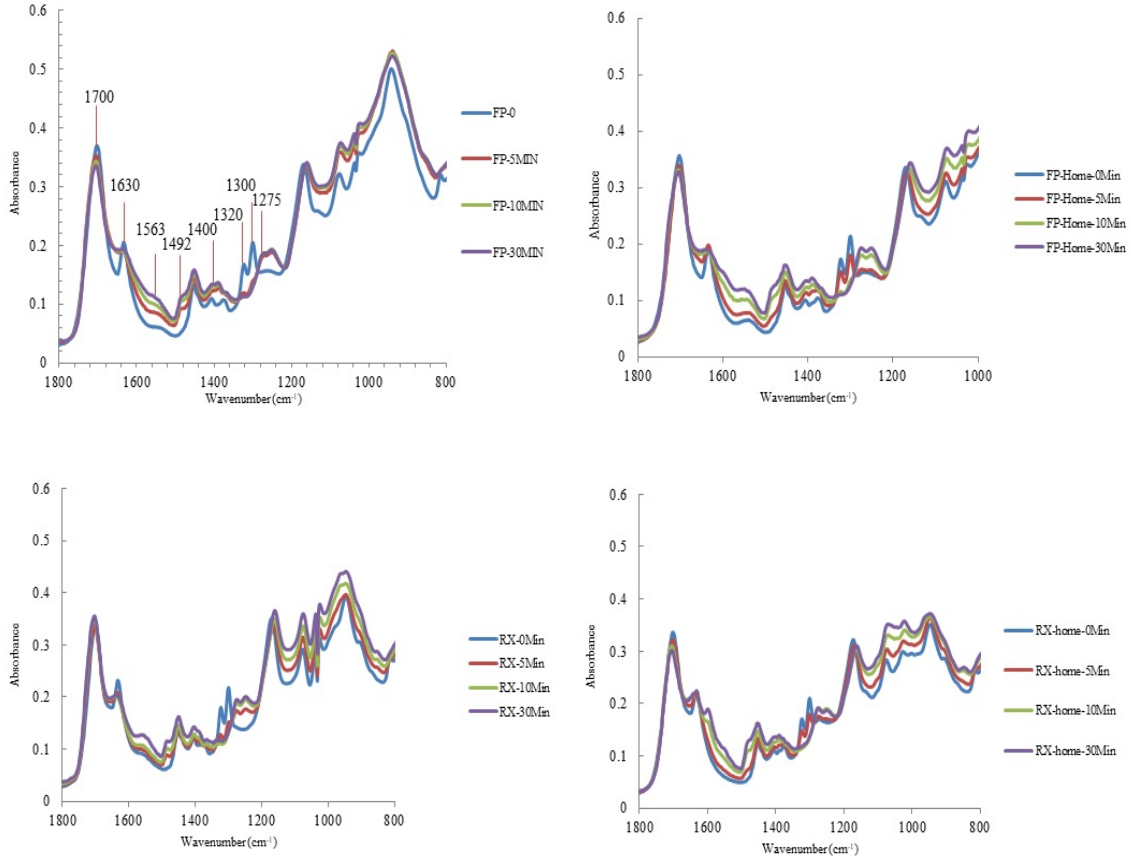

Figure 2 FT-IR spectra of setting reaction at 0, 5, 10 and 30 minutes for a: Commercial FP, b: Home FP, c: Commercial RX and d: Home RX. The peaks highlighted in figure 2a are similar to those found in 2b, 2c and 2d.

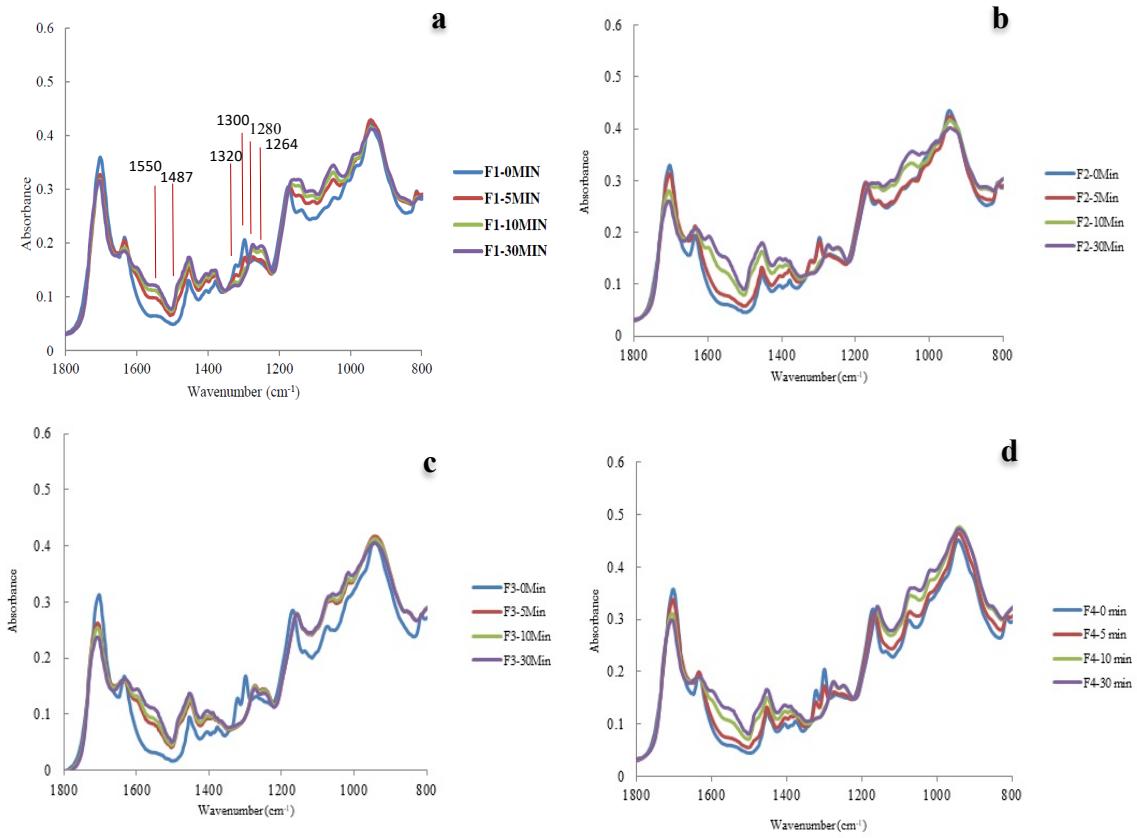

Figure 3 FT-IR spectra of setting reaction at 0, 5, 10 and 30 minutes for a: F1, b: F2, c: F3 and d: F4. The peaks highlighted in figure 2a are similar to those found in 2b, 2c and 2d.

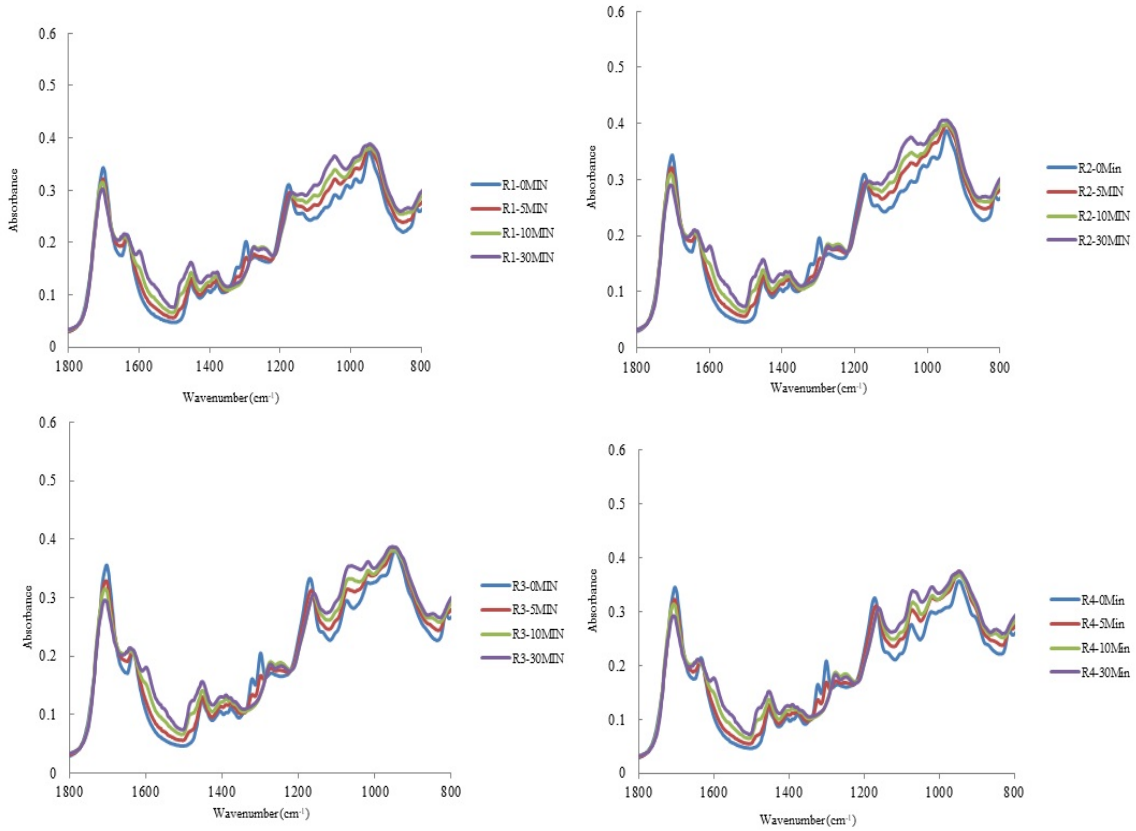

Figure 4 FT-IR spectra of setting reaction at 0, 5, 10 and 30 minutes for a: R1, b: R2, c: R3 and d: R4. The peaks highlighted in figure 2a are similar to those found in 2b, 2c and 2d.

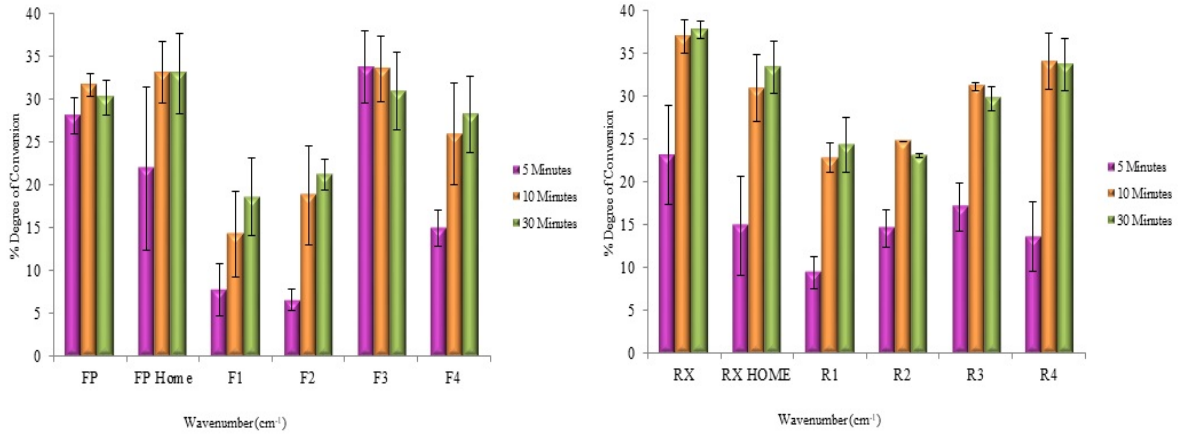

Figure 5 Mean percentage degree of conversion of a: FP and b: RX commercial, home and experimental materials measured at 5, 10 and 30 minutes, calculated from the start of mixing

FTIR Wavenumber (cm^{-1})	Assignment	Component
1020	-OH Ring stretch	HEMA THFM
1059	-OH C-N	HPM UDMA
1086	-OH Ring stretch	HEMA THFM
1250	N-H	UDMA
1300	C-O	Monomer (all three)
1320	C-O	Monomer (all three)
1379	C-H	PAA and monomer (all three)
1405	C-H	PAA and monomer (all three)
1450	C-H	PAA and monomer (all three)
1535	N-H	UDMA
1630	C=C	Monomer (all three)
1630	O-H	Water
1700	C=O	Monomer (all three)

Table 1 RMGIC liquid components FTIR analyses with the corresponding wavenumber (cm^{-1}) and assignment of each component.

Material	Shrinkage strain at 5 minutes % (SD)	Shrinkage strain at 15 minutes % (SD)	Shrinkage strain at 30 minutes % (SD)	Shrinkage strain at 60 minutes % (SD)
FP	1.19 (0.02)	1.34 (0.02)[a]	1.39 (0.02)[a,b]	1.41 (0.02)[a,b]
FP-Home	0.74 (0.06)[a]	1.31 (0.03)[a,b]	1.41 (0.03)[a]	1.46 (0.04)[a]
F1	0.35 (0.07)	0.95 (0.09)	1.12 (0.08)	1.21 (0.09)[c]
F2	0.47 (0.07)	1.19 (0.09)[b,c]	1.31 (0.05)[a,b,c]	1.39 (0.05)[a,b]
F3	0.77 (0.05)[a]	1.21 (0.04)[b,c]	1.28 (0.04)[b,c]	1.32 (0.05)[b,c]
F4	0.72 (0.07)[a]	1.14 (0.09)[c]	1.26 (0.09)[c]	1.35 (0.10)[a,b]

Table 2 Mean percentage shrinkage strain values and standard deviation (SD) at 5, 15, 30 and 60 minutes, from the start of measurement, at 23°C. Similar superscript letters indicates no statistically significant difference between materials at each time point (p>0.05).

Material	Shrinkage strain at 5 minutes % (SD)	Shrinkage strain at 15 minutes % (SD)	Shrinkage strain at 30 minutes % (SD)	shrinkage strain at 60 minutes % (SD)
RX	0.59 (0.19)[a]	1.02 (0.05)[a]	1.07 (0.06)[a,b]	1.12 (0.06)[a,b]
RX-Home	0.23 (0.15)[b]	0.83 (0.11)[b]	0.90 (0.10)[b]	0.96 (0.10)[b]
R1	0.50 (0.07)[a,b]	1.01 (0.06)[a]	1.08 (0.06)[a,b]	1.14 (0.07)[a,b]
R2	0.56 (0.14)[a]	0.97 (0.03)[a,b]	1.03 (0.04)[a,b]	1.09 (0.03)[a,b]
R3	0.43 (0.12)[a,b]	0.94 (0.08)[a,b]	1.02 (0.07)[a,b]	1.08 (0.07)[a,b]
R4	0.51 (0.15)[a]	1.04 (0.16)[a]	1.13 (0.16)[a]	1.20 (0.17)[a]

Table 3 Mean percentage shrinkage strain values and standard deviation (SD) at 5, 15, 30 and 60 minutes from the start of measurement, at 23°C for RX group (commercial, home and experimental). Similar superscript letters indicates no statistically significant difference between materials at each time point (p>0.05).

Material	Shrinkage strain at 5 minutes % (SD)	Shrinkage strain at 15 minutes % (SD)	Shrinkage strain at 30 minutes % (SD)	Shrinkage strain at 60 minutes % (SD)
FP	1.31 (0.05)	1.38 (0.06)[a]	1.41 (0.06)[a]	1.44 (0.07)[a]
FP-Home	1.09 (0.04)[a,b]	1.29 (0.04)[a,b]	1.36 (0.04)[a,b]	1.41 (0.03)[a]
F1	0.94 (0.04)[c,d]	1.18 (0.04)[b,c]	1.25 (0.05)[b]	1.29 (0.05)[a]
F2	1.00 (0.08)[b,d]	1.26 (0.09)[a,b]	1.35 (0.08)[a,b]	1.42 (0.08)[a]
F3	1.19 (0.05)[a]	1.30 (0.05)[a,b]	1.34 (0.05)[a,b]	1.38 (0.05)[a]
F4	0.85 (0.06)[c,d]	1.10 (0.09)[c]	1.24 (0.11)[b]	1.35 (0.14)[a]

Table 4 Mean percentage shrinkage strain values and standard deviation (SD) at 5, 15, 30 and 60 minutes from the start of measurement, at 37°C, for FP group (commercial, home and experimental). Similar superscript letters indicates no statistically significant difference between materials at each time point (p>0.05)

Material	Shrinkage strain at 5 minutes % (SD)	Shrinkage strain at 15 minutes % (SD)	Shrinkage strain at 30 minutes % (SD)	Shrinkage strain at 60 minutes % (SD)
RX	0.95 (0.05)[a,b]	1.07 (0.05)[a,b]	1.11 (0.05)[a,b]	1.16 (0.05)[a,b]
RX-Home	0.97 (0.05)[a,b]	1.06 (0.05)[a,b]	1.11 (0.06)[a,b]	1.17 (0.05)[a,b]
R1	0.98 (0.03)[a,b]	1.07 (0.05)[a,b]	1.13 (0.07)[a,b]	1.19 (0.09)[a,b]
R2	1.04 (0.04)[a]	1.14 (0.04)[a]	1.21 (0.05)[a]	1.27 (0.05)[a]
R3	0.92 (0.02)[b]	1.01 (0.02)[b]	1.07 (0.02)[b]	1.13 (0.03)[b]
R4	0.94 (0.07)[b]	1.07 (0.08)[a,b]	1.14 (0.08)[a,b]	1.20 (0.10)[a,b]

Table 5 Mean percentage shrinkage strain values and standard deviation (SD) at 5, 15, 30 and 60 minutes from the start of measurement, at 37°C for RX group (commercial, home and experimental). Similar superscript letters indicates no statistically significant difference between materials at each time point (p>0.05).

Material	Peak exotherm temperature (SD)	Coefficient of variation CoV	Time at peak exotherm temperature at 23°C (SD)	CoV
FP	3.57 (0.13)	0.04	202.60 (9.71)[c]	0.05
FP-Home	1.46 (0.23)[a]	0.15	258.60 (23.38)[b]	0.09
F1	0.81 (0.12)	0.14	329.40 (14.40)[a]	0.04
F2	1.33 (0.29)[a]	0.22	348.20 (10.71)[a]	0.03
F3	1.85 (0.22)	0.12	285.00 (16.72)[b]	0.06
F4	1.45 (0.11)[a]	0.07	191.40 (15.11)[c]	0.08

Table 6 Polymerisation exotherm and time at exotherm for FP group (commercial, home and experimental), with standard deviations and CoV (n=5 per material), at 23°C. Similar superscript letters indicates no statistically significant difference between materials (p>0.05).

Material	Peak exotherm temperature at 37°C (°C) (SD)	CoV	Time at peak exotherm temperature at 37°C (seconds) (SD)	CoV
FP	6.12 (0.48)	0.08	56.20 (2.28)	0.04
FP-Home	3.01 (0.32)[a]	0.11	81.20 (1.10)[b]	0.01
F1	2.34 (0.16)[b]	0.07	89.80 (6.87)[a]	0.08
F2	2.32 (0.21)[b]	0.09	86.80 (3.19)[a,b]	0.04
F3	3.39 (0.36)[a]	0.11	87.20 (3.35)[a,b]	0.04
F4	2.77 (0.37)[a,b]	0.13	68.00 (3.46)	0.05

Table 7 Polymerisation exotherm and time at exotherm for FP group (commercial, home and experimental) with standard deviations and CoV (n=5 per material), at 37°C. Similar superscript letters indicates no statistically significant difference between materials (p>0.05).

Material	Peak exotherm temperature at 23°C (°C) (SD)	CoV	Time at peak exotherm temperature at 23°C (seconds) (SD)	CoV
RX	1.42 (0.25)[a]	0.18	229.40 (70.37)[a,b]	0.31
RX-Home	0.96 (0.34)[a,b]	0.35	225.00 (65.15)[b,c]	0.29
R1	1.08 (0.21)[a,b]	0.20	309.60 (5.18)[a]	0.02
R2	0.95 (0.35)[a,b]	0.37	144.80 (26.17)[c]	0.18
R3	0.80 (0.22)[b]	0.28	183.20 (29.35)[b,c]	0.16
R4	1.09 (0.17)[a,b]	0.15	156.00 (10.63)[b,c]	0.07

Table 8 Polymerisation exotherm and time at exotherm for RX group (commercial, home and experimental) with standard deviations and CoV (n=5 per material) at 23°C. Similar superscript letters indicates no statistically significant difference between materials (p>0.05).

Material	Peak exotherm temperature at 37°C (°C) (SD)	CoV	Time at Peak exotherm temperature at 37°C (seconds) (SD)	CoV
RX	1.82 (0.28)[a]	0.15	75.40 (13.16)	0.17
RX-Home	1.91 (0.13)[a]	0.07	127.60 (9.48)[a,b]	0.07
R1	1.95 (0.23)[a]	0.12	122.40 (7.20)[b]	0.06
R2	1.93 (0.07)[a]	0.04	133.00 (8.25)[a,b]	0.06
R3	1.94 (0.21)[a]	0.11	115.40 (4.83)[b]	0.04
R4	2.07 (0.15)[a]	0.07	143.40 (12.93)[a]	0.09

Table 9 Polymerisation exotherm and time at exotherm for RX group (commercial, home and experimental) with standard deviations and CoV (n=5 per material) at 37°C. Similar superscript letters indicates no statistically significant difference between materials (p>0.05).